PTPN22 Silencing in the NOD Model Indicates the Type 1 Diabetes–Associated Allele Is Not a Loss-of-Function Variant

Peilin Zheng[1] and Stephan Kissler[1,2]

PTPN22 encodes the lymphoid tyrosine phosphatase (LYP) and is the second strongest non-HLA genetic risk factor for type 1 diabetes. The *PTPN22* susceptibility allele generates an LYP variant with an arginine-to-tryptophan substitution at position 620 (R620W) that has been reported by several studies to impart a gain of function. However, a recent report investigating both human cells and a knockin mouse model containing the R620W homolog suggested that this variation causes faster protein degradation. Whether LYP R620W is a gain- or loss-of-function variant, therefore, remains controversial. To address this issue, we generated transgenic NOD mice (nonobese diabetic) in which *Ptpn22* can be inducibly silenced by RNA interference. We found that *Ptpn22* silencing in the NOD model replicated many of the phenotypes observed in C57BL/6 *Ptpn22* knockout mice, including an increase in regulatory T cells. Notably, loss of *Ptpn22* led to phenotypic changes in B cells opposite to those reported for the human susceptibility allele. Furthermore, *Ptpn22* knockdown did not increase the risk of autoimmune diabetes but, rather, conferred protection from disease. Overall, to our knowledge, this is the first functional study of *Ptpn22* within a model of type 1 diabetes, and the data do not support a loss of function for the *PTPN22* disease variant. ***Diabetes*** **62:896–904, 2013**

PTPN22 encodes the lymphoid tyrosine phosphatase (LYP) (1) that has been shown to modulate the activation of both T and B cells (2,3). *PTPN22* variation is associated with autoimmunity (4–6) and is the second most significant genetic risk factor for type 1 diabetes outside the HLA region (4,7). The *PTPN22* 1858T allele confers susceptibility to autoimmune diabetes because of an arginine to tryptophan substitution at position 620 (R620W) in the LYP protein. The R620W variation disrupts the association of LYP with Csk, a negative regulatory kinase (4), and a model was proposed in which this disruption causes increased phosphatase activity of LYP (8,9). It was suggested that R620W is a gain-of-function variant that dampens activation of T and B cells in response to antigen receptor ligation (3,8,10,11). Diminished signaling was indeed observed in both T and B cells from individuals carrying the 1858T allele (3,8,11). Several hypotheses have proposed how hyporeactivity may affect both T-cell (8) and B-cell (11,12) tolerance. Impaired T-cell receptor signaling could facilitate the escape of autoreactive T cells during thymic selection, impair the selection or activation of regulatory T (Treg) cells, or prevent the peripheral tolerization of autoreactive clones (8). Similarly, B cells may escape tolerance mechanisms by virtue of diminished activation and resistance to apoptosis in response to antigenic stimuli in individuals carrying the 1858T allele (11,12). Although these hypotheses provide a plausible explanation for the association of *PTPN22* variation with autoimmunity, a recent publication reported data incompatible with this model (13). Using human samples and knockin mice carrying the homolog of the human LYP R620W variant (PEST domain-enriched tyrosine phosphatase [PEP] 619W in mouse), this study suggested that the disease variant protein was prone to rapid degradation, making *PTPN22* 1858T a loss-of-function allele. Results from these contradictory studies are difficult to reconcile. Therefore, whether LYP R620W is a gain- or loss-of-function variant remains controversial.

Characterization of *Ptpn22*-deficient C57BL/6 (B6) mice has provided more detailed insights into the role of this gene in lymphocyte function. In mice, *Ptpn22* encodes the LYP homolog PEP. Loss of PEP was shown to facilitate positive selection but to have no impact on negative selection (14). The most notable effect observed in *Ptpn22* knockout (KO) mice was the accumulation of effector/memory T cells (Teff) and their hyperreactivity compared with wild-type (WT) cells. In addition, *Ptpn22* deficiency led to splenomegaly and lymphadenopathy in older mice but without causing autoimmune pathogenesis. A subsequent study showed that these mice also accumulated increased numbers of Treg cells (15), providing a possible explanation for the lack of overt autoimmunity in *Ptpn22*-deficient animals. Moreover, this same study demonstrated that *Ptpn22* KO mice are less susceptible to the experimental autoimmune encephalomyelitis (EAE) model of multiple sclerosis (15). Although the original description of *Ptpn22* KO mice suggested that the loss of this gene may predispose to autoimmunity, the latter report implies, rather, that loss of *Ptpn22* may have an overall protective effect against autoimmune disease.

Because the LYP susceptibility variant R620W was reported to be gain of function (3,8–11), LYP inhibition was proposed as a potential therapeutic approach for type 1 diabetes (8,16). To investigate the function of *PTPN22* in autoimmune diabetes and to evaluate whether inhibition of this gene may protect from disease, we generated transgenic NOD mice (nonobese diabetic) in which *Ptpn22* can be silenced by RNA interference in a doxycycline-dependent manner. Gene silencing recapitulated phenotypic changes observed in *Ptpn22* KO B6 mice. *Ptpn22* knockdown (KD) did not, however, increase the risk of autoimmune diabetes in the NOD model, as would be predicted from the recent report claiming that LYP R620W

From the [1]Rudolf Virchow Center, DFG Research Center for Experimental Biomedicine, University of Würzburg, Würzburg, Germany, and the [2]Joslin Diabetes Center, Harvard Medical School, Boston, Massachusetts.
Corresponding author: Stephan Kissler, stephan.kissler@joslin.harvard.edu.
Received 12 July 2012 and accepted 14 September 2012.
DOI: 10.2337/db12-0929

is a loss-of-function variant. Instead, the findings support the notion that the susceptibility allele of *PTPN22* is a gain-of-function variant.

RESEARCH DESIGN AND METHODS

Mice. All mice were bred and maintained under specific pathogen-free conditions at the University of Würzburg in accordance with institutional guidelines. Lentiviral transgenic P2 and P4 mice were generated as described previously (17). Briefly, lentivirus carrying an inducible short hairpin RNA (shRNA) expression cassette that targets the sequence GATGAGGATTCCAGTTATA (P2) or GCATCTGTACACATCTTTA (P4) in the *Ptpn22* mRNA was microinjected into NOD zygotes. For induction of gene silencing, mice were treated with 200 μg/mL doxycycline in the drinking water, unless otherwise noted. All experiments were approved by the Regional Government of Lower Franconia in accordance with German animal protection laws.

Lentiviral construct for inducible shRNA expression. The inducible shRNA expression system consists of two vectors, pH1tet-flex and FH1t-UTG (provided by Marco J. Herold) (18). The vector pH1tet-flex was digested with the restriction enzymes *Bbs*I and *Xho*I. The backbone was recovered and annealed with P2 or P4 shRNA. The fragment containing the H1 promoter and tet-operator was digested with *Pac*I and inserted into the final vector FH1t-UTG. Positive clones were screened by colony PCR and verified by sequencing.

Luciferase reporter assay. *Ptpn22* cDNA was cloned into the psiCheck2 vector (Promega). 293-F cells were cotransfected with 100 ng psiCheck2 *Ptpn22* reporter construct and 300 ng shRNA-containing vector in the presence or absence of 3 μg/mL doxycycline. Firefly and *Renilla* luciferase activity was measured in cell lysates using a Fluostar Optima luminometer 48 h later.

Quantitative RT-PCR and Western blot. Total RNA was extracted from lymphocytes and reverse-transcribed with a first-strand cDNA synthesis kit (Roche). *Ptpn22* mRNA was quantified with the following primers and Universal Probe Library (UPL) probes (Roche): *1*) *GAPDH*, fwd 5′-agcttgtcatcaacgggaag-3′, rev 5′-tttgatgttagtggggtctcg-3′, UPL probe 9, and *2*) *PTPN22*, fwd 5′-cagaacgtgttcagccaaaa-3′, rev 5′-ttggtcctttgcgttttgaa-3′, UPL probe 17. For the Western blot, lymphocytes were lysed in radioimmunoprecipitation assay buffer supplemented with 10% protease inhibitor cocktail (Sigma-Aldrich) on ice for 30 min. The protein concentration was measured with a bicinchoninic acid protein assay kit (Novagen). Target proteins were probed with the antibodies against PEP (1:1,000) (gift from Andrew C. Chan), actin (1:2,000) (Sigma-Aldrich), and tetracycline repressor (TetR) (1:1,000) (Mobitec).

Flow cytometry. All flow cytometry measurements were performed on a FACSCanto II flow cytometer (BD Biosciences). A FoxP3 staining kit (eBioscience) was used to identify FoxP3$^+$ Treg cells. Data were analyzed using FlowJo software (Tree Star Inc.).

Treg-cell suppression assay. CD4$^+$CD25$^-$ Teff cells and CD4$^+$CD25$^+$ Treg cells were purified by magnetic separation using a CD4$^+$CD25$^+$ isolation kit (Miltenyi Biotech) according to the manufacturer's instructions. CD4-depleted WT splenocytes were irradiated (20 Gy) and used as antigen-presenting cells (2.5×10^5/well). WT CD4$^+$CD25$^-$ Teff cells (2.5×10^4/well) were cocultured with WT or *Ptpn22* KD CD4$^+$CD25$^+$ Treg cells at the indicated ratios and stimulated with 1 μg/mL anti-CD3 antibody in RPMI-1640 medium supplemented with 10% FBS, penicillin/streptomycin, L-glutamine, 2-mercaptoethanol, sodium pyruvate, and HEPES (all from Gibco/Invitrogen).

Treg induction. Naïve CD4$^+$CD62L^{hi} T cells were isolated using a MACS bead kit (Miltenyi Biotech) according to the manufacturer's instructions. Cells were stimulated with 2 μg/mL anti-CD3, 2 μg/mL anti-CD28, and 0.5 ng/mL transforming growth factor-β with or without 1 μg/mL doxycycline. The frequency of FoxP3$^+$ cells was analyzed 72 h later.

Cell transfers. Cells were obtained from WT, P2, and P4 mice (2–4 mice per donor group) pretreated with doxycycline for 1 month. WT cells were mixed with P2 or P4 cells at a 1:1 ratio and transferred into NOD.*scid* mice (severe combined immunodeficiency) (3–4 per group) treated with doxycycline for the duration of the experiment. Cell recipients were dissected 1 month after cell transfer to measure CD44^{hi}CD62L^{lo} T-cell frequencies in lymph nodes and spleen.

Anti-CD3 stimulation in vivo. Ten micrograms anti-CD3 was injected intravenously into WT and transgenic mice pretreated with doxycycline for 10 days. Mice underwent dissection 2 days later for flow cytometry analysis of lymph node cells and splenocytes.

B-cell activation, proliferation, and apoptosis. B cells were purified from splenocytes from mice pretreated with doxycycline for 1 month by positive or negative selection with anti-CD19 or anti-CD43 microbeads (Miltenyi Biotech), respectively. B cells were stimulated with LPS or the indicated concentration of anti-IgM F(ab′)$_2$ or anti-CD40 and stained with anti-CD69, anti-CD25, and 7-aminoactinomycin D (BD Biosciences) 24 h later to measure B-cell activation and apoptosis. For proliferation assays, cells were pulsed with ^{3}H-thymidine (0.5 μCi/well) after 48 h, and thymidine incorporation was measured 16 h later.

Measurement of phospholipase Cγ2 phosphorylation after B-cell activation. B cells were purified from mice pretreated with doxycycline for 1 month. WT and transgenic cells were mixed at a 1:1 ratio to control for interwell variations. B cells were stained with anti-CD19 monoclonal antibody and rested in RPMI-1640 medium at 37°C for 10 min. Aliquots of 0.5×10^6 mixed B cells were transferred to a 96-well plate and activated with 40 μg/mL anti-IgM F(ab′)$_2$ for 1, 3, 5, and 10 min. Cells were immediately fixed with 150 μL Fix Buffer I (BD Biosciences) at 37°C for 10 min, then washed, and permeabilized with Perm Buffer III (BD Biosciences) on ice for 15 min. Cells were stained with phycoerythrin-conjugated anti-phospholipase Cγ2 (PLCγ2) monoclonal antibody (1:200) (pY759; BD Biosciences) at 4°C for 30 min, washed, and analyzed by flow cytometry.

Statistical analyses. All statistical analyses were performed using the Prism software package (GraphPad Software, Inc.). Survival curves were compared using the log-rank test. All other comparisons were performed by unpaired two-tailed *t* test.

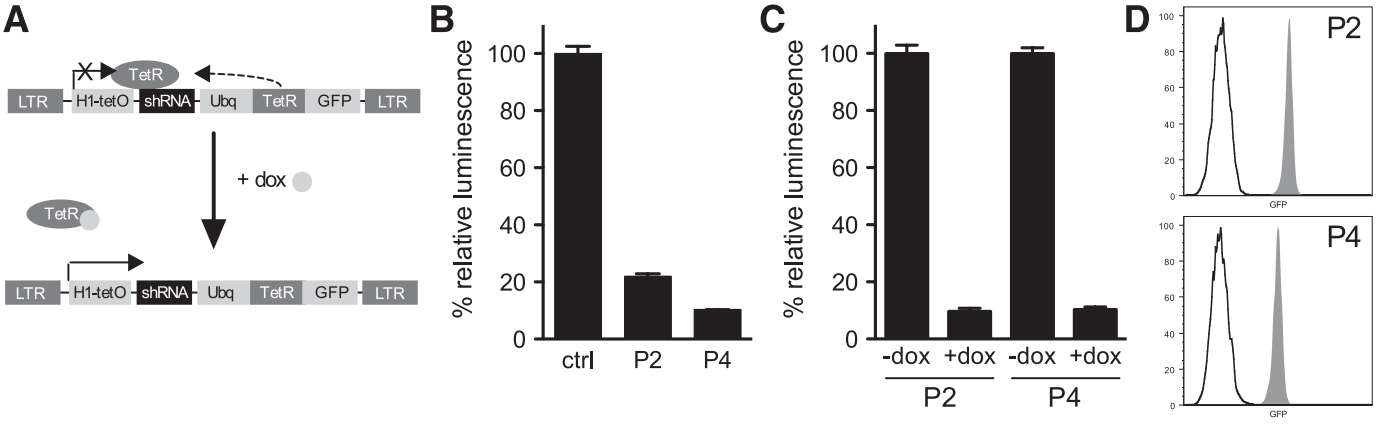

FIG. 1. Generation of inducible *Ptpn22* KD mice. *A*: Schematic representation of the inducible construct used for transgenesis. Long terminal repeats (LTRs) flank a cassette containing a tetracycline-regulated H1 promoter (H1-tetO) driving shRNA expression and a ubiquitin (Ubq) promoter driving expression of the TetR and GFP. Addition of doxycycline (dox) derepresses the H1 promoter and induces shRNA expression. *B*: The silencing efficiency of shRNAs P2 and P4 was validated by cotransfection into 293-F cells of a *Ptpn22* luciferase reporter and lentiviral vectors containing constitutively expressed P2 or P4 shRNA. *C*: 293-F cells were infected with inducible P2 or P4 lentivirus, cultured in the presence or absence of dox, and transfected with the *Ptpn22* luciferase reporter to test for inducibility of the KD constructs. Data in *B* and *C* are representative of two independent experiments. *D:* Representative GFP expression in blood lymphocytes from transgenic P2 and P4 mice. Forward- and side-scatter characteristics were used to gate on the lymphocytic population. Open histogram, nontransgenic; solid histogram, transgenic.

RESULTS

Generation of inducible *Ptpn22* KD NOD mice. To investigate the effect of *PTPN22* gene variation within an experimental model of autoimmunity, we generated NOD mice in which *Ptpn22* can be inducibly silenced. The NOD strain is a widely used model for type 1 diabetes (19), and the spontaneous onset of autoimmunity in this background makes it particularly useful to study genetic factors that contribute to disease risk. We used lentiviral transgenesis to introduce into NOD zygotes a construct encoding an shRNA against *Ptpn22* under the control of a tetracycline-regulatable promoter (FH1t-UTG) (17,18). This lentiviral vector includes the coding sequences for the TetR and green fluorescent protein (GFP) (Fig. 1*A*). To control for possible off-target effects of RNA interference and for insertional effects of the transgene, we generated two transgenic lines with distinct shRNA sequences. We first validated the KD efficiency of several shRNA constructs against *Ptpn22* using a luciferase reporter assay. After identifying two shRNA sequences that potently silenced the *Ptpn22* reporter when expressed from a constitutively active promoter (Fig. 1*B*), we cloned these sequences, termed P2 and P4, into the inducible FH1t-UTG vector (18). We repeated the luciferase reporter assay with cells that had been transduced with the FH1t-P2-UTG or FH1t-P4-UTG lentivirus. We detected potent gene silencing only in cells grown in the presence of the inducing agent doxycycline (Fig. 1*C*), confirming the functionality of these inducible constructs. We proceeded with the generation of two transgenic lines using FH1t-P2-UTG and FH1t-P4-UTG lentivirus and obtained founders for both lines (Fig. 1*D*). These were bred for several generations to generate P2 and P4 mice carrying a single copy of the transgene (verified by Southern blotting of genomic DNA [data not shown]). Potent *Ptpn22* KD was measured both at the mRNA and the protein level in doxycycline-treated but not in untreated transgenic mice (Fig. 2*A* and *B*). Of note, gene silencing was consistently more effective in P2 than in P4 mice (Fig. 2*C*).

***Ptpn22* silencing expands the peripheral Treg-cell compartment.** Transgenic mice were treated with doxycycline for various periods to investigate the effect of *Ptpn22* silencing in adult animals. Although 10–14 days of treatment were sufficient to induce potent *Ptpn22* KD (Fig. 2), we detected no change in the distribution or phenotype of immune cell populations after this short duration of treatment (data not shown). In contrast, prolonged treatment (>1 month) caused a significant increase in the proportion of FoxP3$^+$ Treg cells in secondary lymphoid organs (Fig. 3*A*). To investigate whether the expansion of Treg cells in treated mice affected their function, we tested their activity in vitro and found that *Ptpn22* KD Treg cells remained suppressive (Fig. 3*B*). These results are consistent with observations made in *Ptpn22* KO B6 mice, where Treg cells are similarly increased and retain their suppressive function (15). The Treg-cell increase in secondary lymphoid organs of P2 and P4 mice appeared to be independent of thymic output because the proportion of FoxP3$^+$CD4$^+$CD8$^-$ thymocytes was not affected by gene silencing (Fig. 3*C*), even when *Ptpn22* inhibition was initiated before birth (Fig. 3*D*). To further interrogate the origin of expanded Treg cells in *Ptpn22* KD mice, we quantified the proportion of Helios-expressing FoxP3$^+$CD4$^+$ T cells in doxycycline-treated and -untreated mice (Fig. 3*E*). Helios was reported to be a marker for thymus-derived Treg cells, also known as natural Treg (nTreg) cells (20). Of note, subsequent data from several groups indicated that Helios could be detected in induced Treg (iTreg) cells in some instances (21–23), suggesting that this molecule may not be a reliable marker to differentiate nTreg from iTreg. Notwithstanding, because we found no change in the proportion of Helios$^+$ Treg cells in the periphery of *Ptpn22* KD mice, we interpret our data as signifying that no Treg subpopulation, whether Helios expressing or not, is preferentially expanded after *Ptpn22* silencing. We also tested whether the loss of *Ptpn22* affected the propensity of naïve T cells to convert into

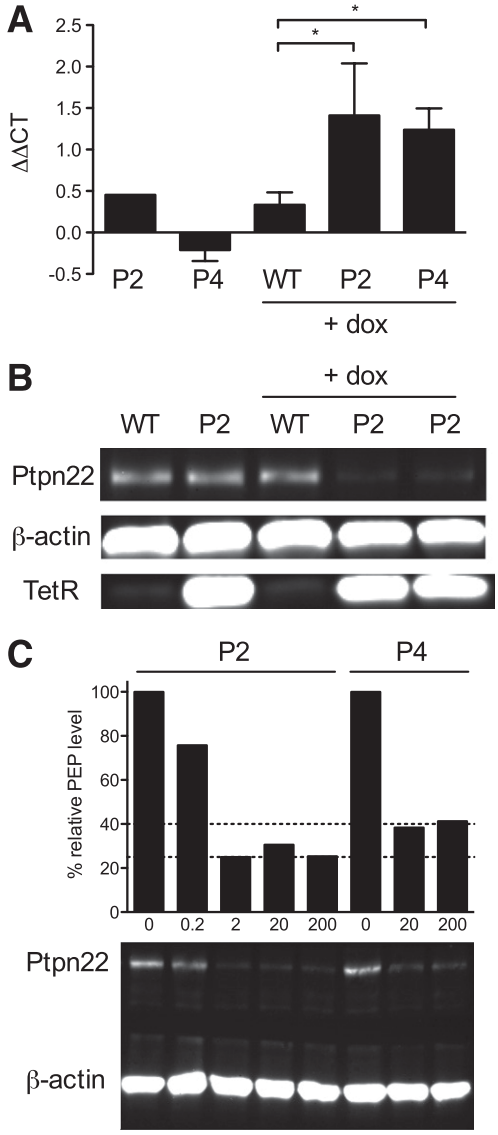

FIG. 2. Validation of *Ptpn22* silencing in transgenic P2 and P4 mice. *A*: Quantitation of *Ptpn22* mRNA levels in lymphocytes from untreated P2 and P4 mice and from doxycycline (dox)-treated WT, P2, and P4 mice relative to *Ptpn22* expression in untreated WT mice. ΔΔCTs (ΔCT of sample – ΔCT untreated WT such that an increase in ΔΔCT indicates lower mRNA levels) are shown. Data were averaged from four independent experiments. *B*: Quantitation of PEP (Ptpn22) protein by Western blotting in lymphocytes from untreated or dox-treated (200 μg/mL) WT and P2 mice. TetR was also assayed to verify transgene expression. *C:* Quantitation of PEP protein in lymphocytes after exposure to increasing doses of dox (μg/mL) for both P2 and P4 mice. Data in *B* and *C* are representative of six and two similar experiments, respectively. All mice were 8–12 weeks old and had received dox for 10–14 days. *$P < 0.05$. CT, cycle threshold.

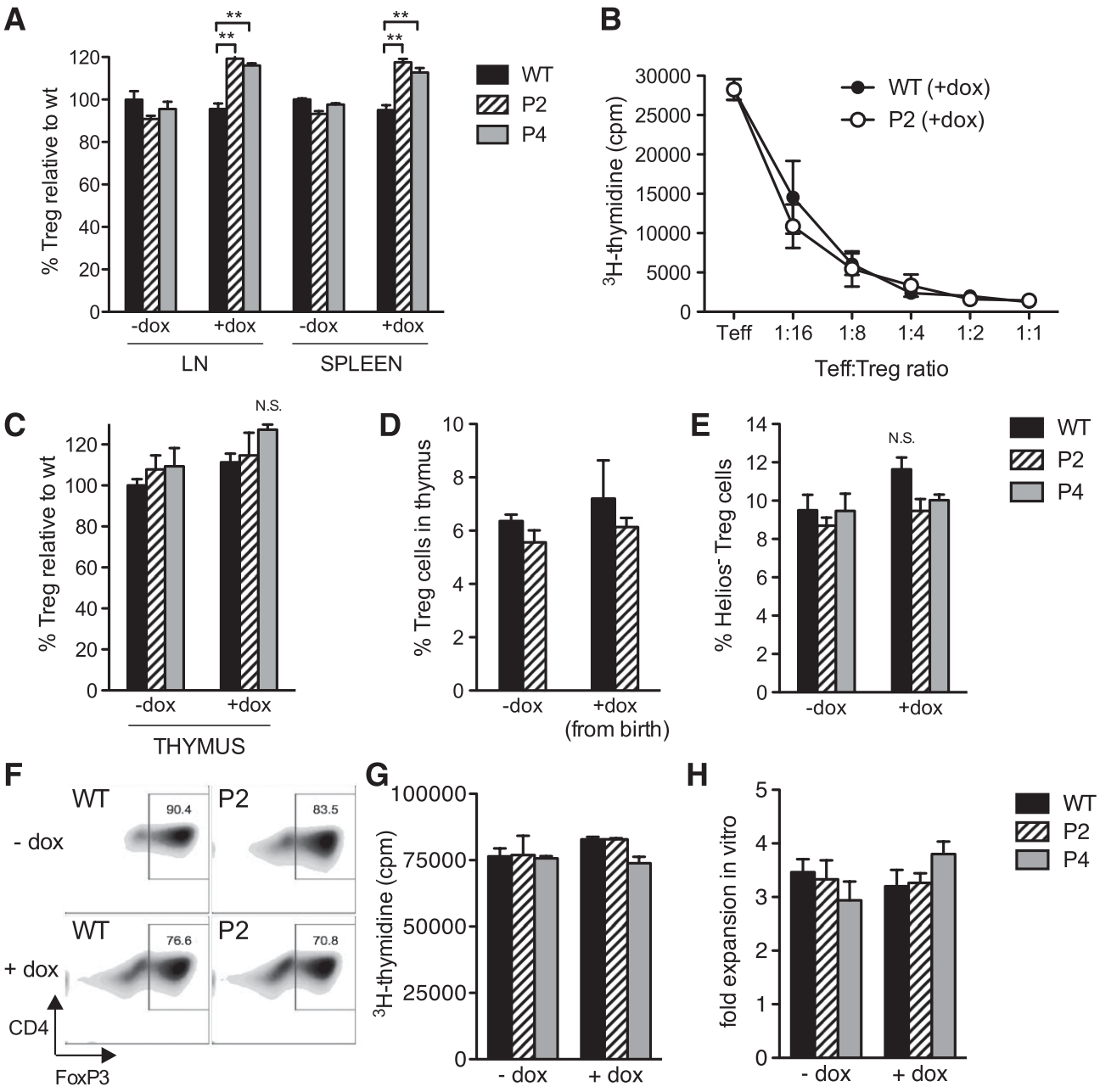

FIG. 3. ***Ptpn22*** **silencing increases peripheral but not thymic Treg-cell numbers.** ***A:*** **The percentage of FoxP3$^+$CD4$^+$ T cells in lymph nodes (LNs) or spleen of untreated or doxycycline (dox)-treated (for 4 weeks from the age of 8 weeks) WT, P2, and P4 mice relative to untreated WT (LN 11.23%, spleen 16.7%). Data were averaged from three mice per group and are representative of 13 similar experiments.** ***B*****: Proliferation of WT CD4$^+$CD25$^-$ T cells in response to anti-CD3 stimulation was measured in the presence or absence of CD4$^+$CD25$^+$ T cells from WT or P2 mice treated with dox for 2 weeks from the age of 8 weeks. Data are mean ± SEM of triplicates and are representative of three independent experiments.** ***C*****: The percentage FoxP3$^+$CD4$^+$CD8$^-$ T cells in the thymus of untreated or dox-treated (as in** ***A*****) WT, P2, and P4 mice relative to untreated WT (7.27%).** ***D*****: The percentage FoxP3$^+$CD4$^+$CD8$^-$ T cells in the thymus of untreated or dox-treated (for 2 months from birth) WT, P2, and P4 mice.** ***E*****: The percentage of Helios-negative cells among FoxP3$^+$CD4$^+$ T cells in lymph nodes from untreated or dox-treated (as in** ***A*****) WT, P2, and P4 mice. Data in** ***C, D,*** **and** ***E*** **were averaged from three to four mice per group and are representative of five (*** ***C*** **and** ***E*** **) and two (*** ***D*** **) similar experiments.** ***F*****: CD62L^{hi}CD4$^+$ T cells from untreated or dox-treated (for 2 weeks from 8 weeks of age) WT and P2 mice were activated in the presence of transforming growth factor-β (with or without dox) for 3 days before measuring FoxP3 expression. Data are representative of two independent experiments.** ***G*** **and** ***H:*** **Proliferation at 72 h (*** ***G*** **) and fold numerical expansion after 10 days in culture (*** ***H*** **) of Treg cells from dox-treated (for 2 weeks from 6 weeks of age) or untreated WT, P2, and P4 mice after stimulation with CD3- and CD28-antibody–coated beads; data are mean ± SEM of triplicate measurements. *****P*** **< 0.01. NS, not significant at** ***P*** **> 0.05.**

FoxP3-expressing Treg cells as a thymus-independent explanation for the increase in Treg cells observed after gene silencing. However, naïve CD4$^+$CD62L^{hi} T cells from WT and *Ptpn22* KD mice did not differ in their potential for Treg conversion in vitro (Fig. 3*F*). Furthermore, we did not detect any difference in the acute proliferative behavior of Treg cells in vitro after *Ptpn22* silencing (Fig. 3*G* and *H*). The data suggest that the entire peripheral Treg-cell compartment is expanded by loss of *Ptpn22* and that neither thymic output of nTreg nor conversion of naïve T cells into iTreg cells is responsible for this expansion in *Ptpn22* KD mice.

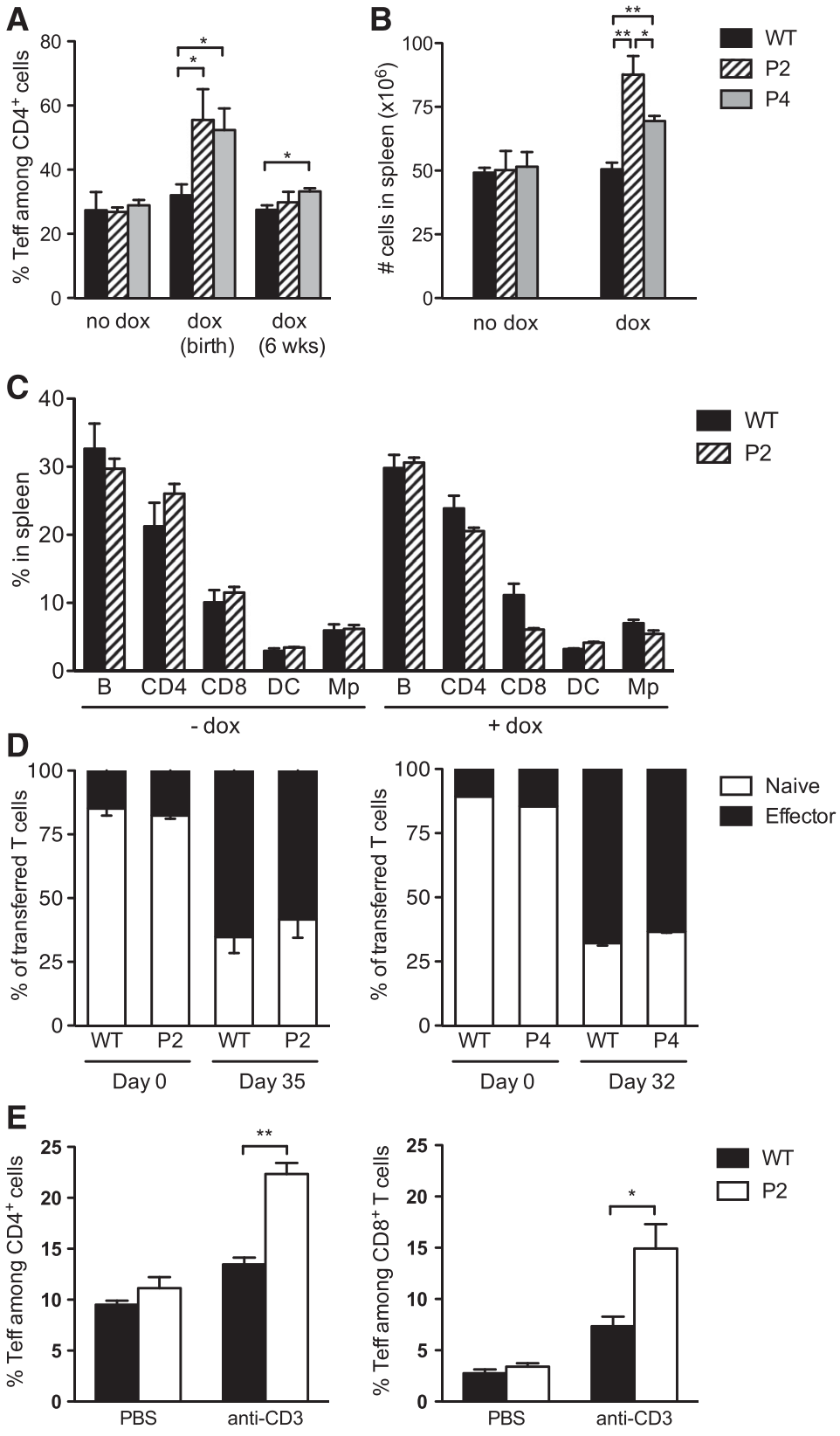

FIG. 4. Time of treatment determines the effect of *Ptpn22* silencing on Teff-cell differentiation. *A*: The percentage CD44^{hi}CD62L^{lo} (Teff) cells within the CD4^{+} T-cell compartment were quantified in WT, P2, and P4 mice that had either been untreated, treated for 2 months from birth, or treated for 3 months from the age of 6 weeks. Data for CD8^{+} T cells were similar (not shown). Data are averaged (mean ± SEM) for two to six mice per group and are representative of two (doxycycline [dox] from birth) and six (dox from 6 weeks) similar experiments. *B*: Cellularity of spleens from WT, P2, and P4 mice untreated or treated with dox for 4–5 months from the age of 10 weeks averaged (mean ± SEM) for 14 WT, 5 P2, and 8 P4 mice (untreated groups) and 19 WT, 10 P2, and 9 P4 mice (treated groups). *C*: Relative distribution of B cells, CD4 and CD8 T cells, dendritic cells (DC), and macrophages (Mp) in the spleen of WT and P2 mice either untreated or treated from the age of 4 weeks for a duration of 4 months. Data are averaged (mean ± SEM) from five mice per group and representative of four similar experiments. *D:* Quantification of naïve (CD44^{lo}CD62L^{hi})

Time of treatment determines the effect of *Ptpn22* silencing on Teff-cell differentiation. The loss of *Ptpn22* in gene-deficient B6 mice was shown to cause a significant expansion of Teff cells in older mice (14). In *Ptpn22* KD mice, a similar increase in $CD44^{hi}CD62L^{lo}$ T cells was apparent when gene silencing was induced from birth (Fig. 4*A*). In contrast, even though induction of *Ptpn22* silencing in adult mice for a duration of several months caused significant splenomegaly (Fig. 4*B*), expansion of the Teff-cell compartment was almost undetectable after delayed gene silencing (Fig. 4*A*). The overall distribution of lymphocyte populations in the spleen of treated mice was not significantly altered, suggesting that homeostasis of both T and B cells was increased by *Ptpn22* inhibition (Fig. 4*C*), although this effect was markedly weaker in the $CD8^+$ T-cell compartment. Using two different strategies, we tested the propensity of naïve T cells to differentiate into Teff cells more directly. First, we transferred a mixture of WT and transgenic $CD4^+$ T cells into NOD.*scid* recipients and examined the fate of these cells 1 month after transfer. In this setting, T cells from *Ptpn22* KD animals did not differ from WT cells in their propensity to differentiate into Teff cells (Fig. 4*D*). In contrast, when we injected WT or transgenic mice with anti-CD3 antibody, we found that *Ptpn22* silencing greatly promoted the activation and differentiation of T cells after this stimulus (Fig. 4*E*). The difference between these two experiments may be accounted for by the fact that the acquisition of an effector phenotype following lymphopenia-induced expansion likely differs from that caused by a strong T-cell receptor stimulus, such as anti-CD3. The data thus confirm that *Ptpn22* modulates the propensity of naïve cells to differentiate into Teff cells but suggest that the increase of Teff cells observed in *Ptpn22* KO mice largely depends on altered thymic selection in early stages of development when thymic output is most influential on the peripheral T-cell repertoire. Our inducible system demonstrates that *Ptpn22* inhibition in adult animals has a lesser impact on the differentiation of naïve T cells into Teff cells, at least under homeostatic conditions. This contrasts with effects on Treg cells that were detectable irrespective of the timing of *Ptpn22* silencing.

B-cell activation and apoptosis are increased by *Ptpn22* silencing. Characterization of *Ptpn22* KO mice had revealed an increase in serum antibody titers (14), albeit no increase in autoantibodies and no detailed analysis of B-cell function have been reported from these mice to date. In humans, B cells from carriers of the *PTPN22* susceptibility allele display decreased activation (3,10,11) and resistance to apoptosis (11). In addition, LYP R620W was found to reduce Syk, Akt, and PLCγ2 phosphorylation after B-cell receptor ligation (11), which would be consistent with a gain of function of this variant. In light of these observations, we sought to directly correlate loss of PEP activity with B-cell function using *Ptpn22* KD mice. *Ptpn22* silencing increased the upregulation of both CD25 and CD69 in B cells after anti-IgM stimulation (Fig. 5*A*). Furthermore, a higher fraction of B cells became $CD25^+CD69^+$ in response to both anti-IgM and anti-CD40 when *Ptpn22* expression was inhibited (Fig. 5*B*). At the same time, *Ptpn22* KD B cells displayed decreased survival in culture compared with WT cells (Fig. 5*C*). Although cells from P2 and P4 mice were concordant in most respects, the difference in KD efficiency between these two transgenic lines became most apparent when B-cell proliferation was quantified after in vitro stimulation (Fig. 5*D*). B cells from P2 mice proliferated more vigorously than cells from both WT and P4 animals in response to both anti-IgM and anti-CD40. Similarly, B cells from P2 mice displayed increased phosphorylation of PLCγ2, but *Ptpn22* silencing in P4 cells was insufficient to effect a detectable change in PLCγ2 phosphorylation (Fig. 5*E*). These combined results demonstrate that the inhibition of *Ptpn22* has the exact opposite effect on B-cell signaling compared with the human R620W variant, which decreases activation and PLCγ2 phosphorylation and increases survival in response to stimulation (3,10,11).

***Ptpn22* silencing protects P2 mice from autoimmune diabetes.** Based on evidence that disease-associated LYP R620W is a gain-of-function variant, it was suggested that LYP inhibition may protect against autoimmunity (8). Even though the *PTPN22* variation does not associate with multiple sclerosis, PEP deficiency was recently found to reduce the severity of EAE (15). The generation of an inducible *Ptpn22* KD model was aimed at evaluating the therapeutic potential of *Ptpn22* inhibition with a more clinically relevant approach. The absence of PEP throughout development in gene-deficient mice causes changes in thymic selection. The ensuing effects on the developing immune system likely differ from alterations in cell function caused by the acute inhibition of *Ptpn22* in mature lymphocytes. We therefore opted to initiate *Ptpn22* silencing in adult animals to better mimic a therapeutic intervention by LYP inhibition. To this end, we measured the frequency of diabetes in transgenic mice and their WT littermates that either had been left untreated or received doxycycline from the age of 10 weeks. Doxycycline-treated P2 but not P4 mice were significantly protected from diabetes compared with both untreated mice and treated WT mice (Fig. 6*A* and *B*). Disease frequency did not differ among untreated P2, P4, and WT mice. P4 mice showed no protection from disease, even when treated from an earlier time point of 4 weeks of age (Fig. 6*C*). We speculate that the weaker *Ptpn22* KD in P4 mice may explain the difference in disease susceptibility between the two transgenic lines. This would be consistent with our observation that P4 lymphocytes showed less marked differences from the WT phenotype than P2 cells. Even though this difference in disease susceptibility may need to be resolved, it is apparent that *Ptpn22* inhibition did not increase the risk of autoimmune diabetes in either transgenic line, contrary to what would be predicted from a study claiming that R620W is a loss-of-function variant (13). Instead, consistent with results in the EAE model (15), *Ptpn22* silencing protected from autoimmune pathology.

DISCUSSION

After the discovery of the *PTPN22* association with autoimmune diabetes, several groups carried out functional

and effector ($CD44^{hi}CD62L^{lo}$) cells in mixed WT and P2 or WT and P4 $CD4^+$ T-cell populations before and after (32–35 days) transfer into NOD.*scid* mice. WT and transgenic cells were identified on the basis of GFP expression. *E*: The percentage of $CD44^{hi}CD62L^{lo}$ (Teff) cells was quantified in $CD4^+$ and $CD8^+$ T cells from WT and P2 mice (pretreated with dox for 10 days) 2 days after injection with PBS only or anti-CD3 antibody 10 μg. Data in *D* and *E* are averaged from three to four mice per group and representative of two independent experiments each. *$P < 0.05$; **$P < 0.01$.

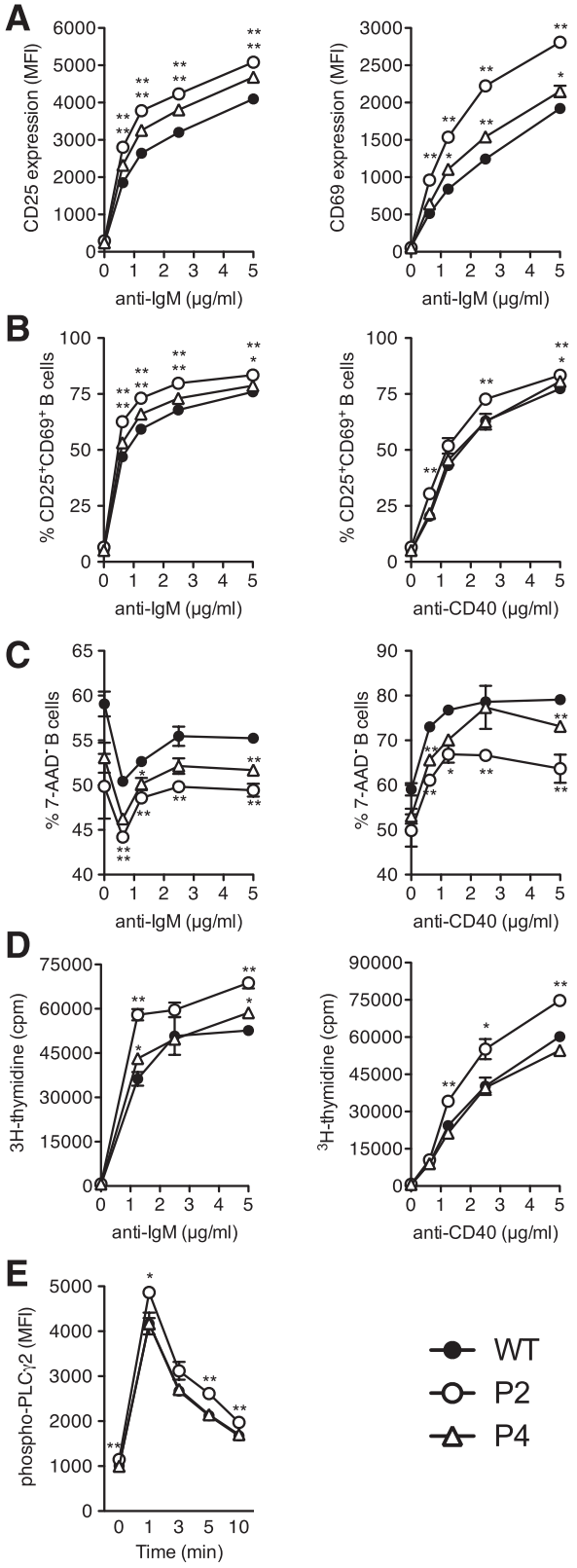

FIG. 5. *Ptpn22* silencing increases activation and decreases survival of transgenic B cells. B cells from WT, P2, and P4 mice treated with doxycycline for 4 weeks from 8 weeks of age were stimulated with anti-IgM (*A–E*) or anti-CD40 (*B–D*) at the indicated concentration. Mean fluorescence intensity (MFI) of CD25 and CD69 staining (*A*), percentage of $CD25^+CD69^+$ cells (*B*), and percentage of 7-aminoactinomycin D negative ($7\text{-}AAD^-$) (nonapoptotic) cells (*C*) were quantified 24 h after stimulation. Proliferation was measured by ^{3}H-thymidine incorporation 48 h poststimulation (*D*). The phosphorylation of PLCγ2 was measured at a single concentration of anti-IgM (40 μg/mL) at the indicated time poststimulation (*E*). Data are representative of four (*A–C*), seven (*D*), and two (*E*) independent experiments. Data are mean ± SEM of triplicate measurements. *$P < 0.05$; **$P < 0.01$.

studies with lymphocytes from individuals who carry the susceptibility variant and found evidence that the disease allele is a gain-of-function variant (3,8–11). Data from animal models did not unequivocally support these findings because *Ptpn22* KO mice appear to present signs of lymphocyte activity predisposing to autoimmunity (14). Furthermore, combining *Ptpn22* deficiency with a mutant allele of CD45 caused lupus-like autoimmunity in double-mutant mice, and this evidence was interpreted as the disease allele being a loss-of-function variant (24). Finally, a notable study published in 2011 suggested that the *PTPN22* disease variant encodes an LYP protein that is more prone to degradation than the protective variant. Knockin of a mutant *Ptpn22* allele that encodes PEP 619W, the homolog of human LYP R620W, caused a phenotype reminiscent of *Ptpn22* KO (13). However, despite an accumulation of Teff cells and increased serum antibody levels, *Ptpn22* KO mice do not develop any signs of overt autoimmunity (14) possibly because of an increase in Treg-cell numbers (15). The present data from *Ptpn22* KD NOD mice confirm that the peripheral Treg-cell compartment is increased in the absence of PEP. In contrast to *Ptpn22* KO B6 mice, however, transgenic NOD mice did not have a higher proportion of $FoxP3^+$ thymocytes. We observed in NOD mice that the expansion of Treg cells caused by the loss of PEP can occur independently of thymic output, indicating that *Ptpn22* plays a role in the peripheral homeostasis of Treg cells. Of note, Treg-cell numbers in *Ptpn22* KO mice were more substantially increased than in our KD model, and this may be due to both the incomplete loss of PEP in *Ptpn22* KD mice and the additive effect in KO mice of greater thymic output together with direct effects on peripheral Treg cells. In this regard, however, it has been reported that a significant proportion of $FoxP3^+$ cells found in the thymus is not recently generated but may in fact represent either long-term resident cells or cells that have recirculated into the thymus from the periphery (25,26). In light of the recent observation that the homeostasis of thymic resident Treg cells depends on signals distinct from those governing Treg-cell development (26), this raises the possibility that the increased Treg-cell population observed in the thymus of *Ptpn22* KO mice (15) may in fact be a consequence of the expansion of the mature Treg-cell compartment.

How *Ptpn22* silencing exerts its effect on peripheral Treg cells is not entirely clear, but we suggest that conversion of naïve T cells into iTreg cells is not involved. First, we did not observe increased efficiency of Treg conversion in vitro after *Ptpn22* silencing, and second, the proportion of Helios-negative $FoxP3^+$ cells [presumed nonthymic Treg cells (20), although some iTreg cells may also express Helios (21–23)] was not altered after Treg-cell expansion. Loss of PEP did not change the acute proliferative behavior of Treg cells but may instead increase homeostatic T-cell receptor signals essential for their peripheral maintenance and could decrease their requirement for IL-2 (27), allowing expansion of the Treg-cell niche. Alternatively, IL-2 levels may increase as a consequence of facilitated differentiation and activation of Teff cells and/or other immune cells producing IL-2, and loss of

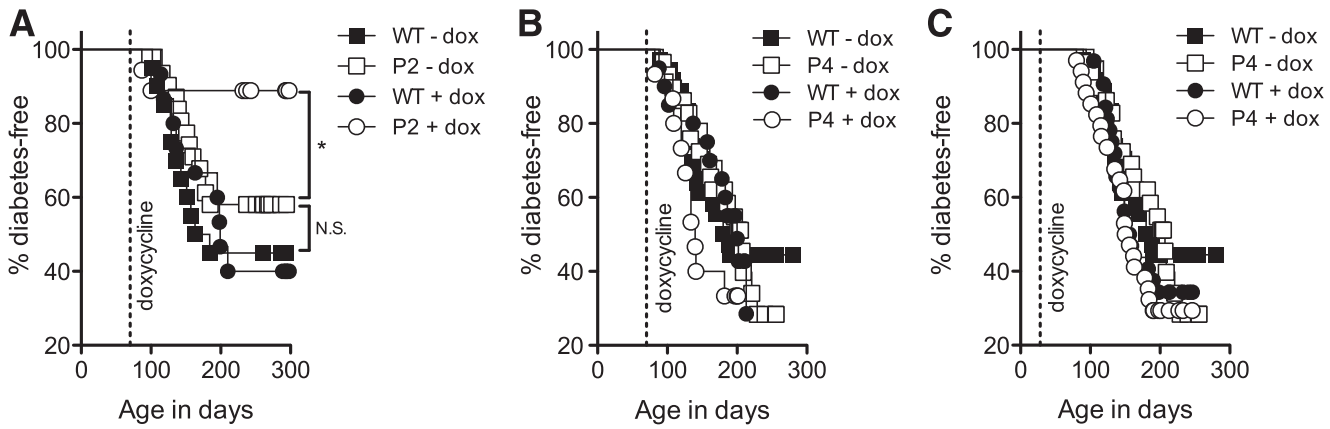

FIG. 6. P2 but not P4 mice are protected from autoimmune diabetes by *Ptpn22* silencing. Female P2 (*A*) and P4 (*B* and *C*) transgenic mice and their WT littermates were either left untreated or treated with doxycycline (dox) (200 μg/mL drinking water) from the age of 10 weeks (*A* and *B*) or 4 weeks (*C*). The dashed line indicates start of treatment. *A*: WT – dox (n = 20), P2 – dox (n = 31), WT + dox (n = 15), P2 + dox (n = 18). *B*: WT – dox (n = 36), P4 – dox (n = 29), WT + dox (n = 20), P4 + dox n = 15. *C*: WT – dox n = 36, P4 – dox n = 29, WT + dox n = 32, P4 + dox n = 34. Log-rank test for *A*: WT – dox versus P2 – dox P = 0.26, WT + dox versus P2 + dox P = 0.006, P2 – dox versus P2 + dox P = 0.0418 (*). NS, not significant.

Ptpn22 could thereby promote Treg-cell expansion in a cell-extrinsic manner.

Although neither the present study nor the previous report demonstrating expansion of Treg cells in *Ptpn22*-deficient animals showed a direct link between this expansion and protection from autoimmunity, it is tempting to speculate a causal effect. Both protection from EAE in *Ptpn22* KO mice and protection from autoimmune diabetes in P2 NOD mice shown here may be imparted by a more potent Treg-cell compartment.

Unlike its effect on Treg cells, *Ptpn22* KD modulation of Teff-cell differentiation seemed to take effect primarily at the level of thymic development. Treatment of *Ptpn22* KD mice from birth had a vastly more significant outcome than gene silencing initiated in adult mice. This may be explained by changes in positive selection described previously (14). Alterations of thymic selection can be predicted to have a lesser impact on the peripheral T-cell repertoire once thymic output starts waning (i.e., in adult animals).

Further, our work demonstrates that loss of *Ptpn22* causes hyperreactivity and decreases survival of B cells. Because B cells are essential for the full penetrance of autoimmune diabetes in NOD mice (28), a defect in B-cell function may synergize with increased Treg-cell numbers in reducing the risk of autoimmune diabetes. In this context, it is of interest that the lack of protection observed in P4 mice correlates with a lesser dysfunction of B cells in vitro, and further work will be required to determine the relative contributions of the Treg- and B-cell compartments to the protected disease phenotype of P2 mice.

Data reported for B cells from individuals carrying the *PTPN22* susceptibility allele are contradictory (10–13). The phenotype of *Ptpn22* KD B cells presented here is the exact opposite of observations made for R620W by groups suggesting a gain of function (10,11) yet matches data obtained for this variant by the group proposing a loss of function (13). Consequently, we cannot draw an unequivocal conclusion about what functional change the human disease variant may cause based solely on cellular phenotypes. However, because we did not observe disease exacerbation after *Ptpn22* inhibition, the findings are difficult to reconcile with the hypothesis that the *PTPN22* disease allele is a loss-of-function variant caused by accelerated degradation of LYP (13). Instead, the results are most consistent with LYP R620W being a gain-of-function variant. In conclusion, we suggest that the present study of *Ptpn22* inhibition in the NOD mouse model supports earlier claims that the susceptibility allele of *PTPN22* is a gain-of-function variant and that inhibition of LYP may have therapeutic value for the treatment of autoimmunity.

ACKNOWLEDGMENTS

P.Z. was supported by a grant from the German Excellence Initiative to the Graduate School of Life Sciences of the University of Würzburg. This work was funded by the Deutsche Forschungsgemeinschaft (FZ82) and by a Career Development Award from the Juvenile Diabetes Research Foundation (2-2010-383) to S.K. The funder played no role in the conduct of the study, collection of data, management of the study, analysis of data, interpretation of data, or preparation of the manuscript.

No potential conflicts of interest relevant to this article were reported.

P.Z. designed and performed all experiments, analyzed data, and gave input on the manuscript. S.K. conceived and supervised the project, analyzed data, and wrote the manuscript. S.K. is the guarantor of this study and, as such, had full access to all the data in the study and takes responsibility for the integrity of the data and the accuracy of the data analysis.

Parts of this study were presented in poster form at the 12th International Congress of the Immunology of Diabetes Society, Victoria, British Columbia, Canada, 15–19 June 2012.

The authors thank Nicole Hain, University of Würzburg, for expert technical assistance and Julie Joseph, University of Würzburg, for help with cell preparations in large-scale experiments. The authors also thank Marco J. Herold, Walter and Eliza Hall Institute of Medical Research, for the pH1t-flex and FH1t-UTG vectors and Andrew C. Chan, Genentech, for the anti-PEP antibody.

REFERENCES

1. Cohen S, Dadi H, Shaoul E, Sharfe N, Roifman CM. Cloning and characterization of a lymphoid-specific, inducible human protein tyrosine phosphatase, Lyp. Blood 1999;93:2013–2024

2. Cloutier JF, Veillette A. Cooperative inhibition of T-cell antigen receptor signaling by a complex between a kinase and a phosphatase. J Exp Med 1999;189:111–121
3. Rieck M, Arechiga A, Onengut-Gumuscu S, Greenbaum C, Concannon P, Buckner JH. Genetic variation in PTPN22 corresponds to altered function of T and B lymphocytes. J Immunol 2007;179:4704–4710
4. Bottini N, Musumeci L, Alonso A, et al. A functional variant of lymphoid tyrosine phosphatase is associated with type I diabetes. Nat Genet 2004;36: 337–338
5. Kyogoku C, Langefeld CD, Ortmann WA, et al. Genetic association of the R620W polymorphism of protein tyrosine phosphatase PTPN22 with human SLE. Am J Hum Genet 2004;75:504–507
6. Vang T, Miletic AV, Bottini N, Mustelin T. Protein tyrosine phosphatase PTPN22 in human autoimmunity. Autoimmunity 2007;40:453–461
7. Barrett JC, Clayton DG, Concannon P, et al.; Type 1 Diabetes Genetics Consortium. Genome-wide association study and meta-analysis find that over 40 loci affect risk of type 1 diabetes. Nat Genet 2009;41:703–707
8. Vang T, Congia M, Macis MD, et al. Autoimmune-associated lymphoid tyrosine phosphatase is a gain-of-function variant. Nat Genet 2005;37:1317–1319
9. Fiorillo E, Orrú V, Stanford SM, et al. Autoimmune-associated PTPN22 R620W variation reduces phosphorylation of lymphoid phosphatase on an inhibitory tyrosine residue. J Biol Chem 2010;285:26506–26518
10. Arechiga AF, Habib T, He Y, et al. Cutting edge: the PTPN22 allelic variant associated with autoimmunity impairs B cell signaling. J Immunol 2009; 182:3343–3347
11. Habib T, Funk A, Rieck M, et al. Altered B cell homeostasis is associated with type I diabetes and carriers of the PTPN22 allelic variant. J Immunol 2012;188:487–496
12. Menard L, Saadoun D, Isnardi I, et al. The PTPN22 allele encoding an R620W variant interferes with the removal of developing autoreactive B cells in humans. J Clin Invest 2011;121:3635–3644
13. Zhang J, Zahir N, Jiang Q, et al. The autoimmune disease-associated PTPN22 variant promotes calpain-mediated Lyp/Pep degradation associated with lymphocyte and dendritic cell hyperresponsiveness. Nat Genet 2011;43:902–907
14. Hasegawa K, Martin F, Huang G, Tumas D, Diehl L, Chan AC. PEST domain-enriched tyrosine phosphatase (PEP) regulation of effector/memory T cells. Science 2004;303:685–689
15. Maine CJ, Hamilton-Williams EE, Cheung J, et al. PTPN22 alters the development of regulatory T cells in the thymus. J Immunol 2012;188:5267–5275
16. Vang T, Liu WH, Delacroix L, et al. LYP inhibits T-cell activation when dissociated from CSK. Nat Chem Biol 2012;8:437–446
17. Kissler S, Stern P, Takahashi K, Hunter K, Peterson LB, Wicker LS. In vivo RNA interference demonstrates a role for Nramp1 in modifying susceptibility to type 1 diabetes. Nat Genet 2006;38:479–483
18. Herold MJ, van den Brandt J, Seibler J, Reichardt HM. Inducible and reversible gene silencing by stable integration of an shRNA-encoding lentivirus in transgenic rats. Proc Natl Acad Sci U S A 2008;105:18507–18512
19. Anderson MS, Bluestone JA. The NOD mouse: a model of immune dysregulation. Annu Rev Immunol 2005;23:447–485
20. Thornton AM, Korty PE, Tran DQ, et al. Expression of Helios, an Ikaros transcription factor family member, differentiates thymic-derived from peripherally induced Foxp3+ T regulatory cells. J Immunol 2010;184:3433–3441
21. Verhagen J, Wraith DC. Comment on "Expression of Helios, an Ikaros transcription factor family member, differentiates thymic-derived from peripherally induced Foxp3+ T regulatory cells". J Immunol 2010;185:7129; author reply 7130
22. Gottschalk RA, Corse E, Allison JP. Expression of Helios in peripherally induced Foxp3+ regulatory T cells. J Immunol 2012;188:976–980
23. Akimova T, Beier UH, Wang L, Levine MH, Hancock WW. Helios expression is a marker of T cell activation and proliferation. PLoS ONE 2011;6:e24226
24. Zikherman J, Hermiston M, Steiner D, Hasegawa K, Chan A, Weiss A. PTPN22 deficiency cooperates with the CD45 E613R allele to break tolerance on a non-autoimmune background. J Immunol 2009;182:4093–4106
25. McCaughtry TM, Wilken MS, Hogquist KA. Thymic emigration revisited. J Exp Med 2007;204:2513–2520
26. Cuss SM, Green EA. Abrogation of CD40-CD154 signaling impedes the homeostasis of thymic resident regulatory T cells by altering levels of IL-2, but does not affect regulatory T cell development. J Immunol 2012;189: 1717–1725
27. Josefowicz SZ, Lu L-F, Rudensky AY. Regulatory T cells: mechanisms of differentiation and function. Annu Rev Immunol 2012;30:531–564
28. Serreze DV, Chapman HD, Varnum DS, et al. B lymphocytes are essential for the initiation of T cell-mediated autoimmune diabetes: analysis of a new "speed congenic" stock of NOD.Ig mu null mice. J Exp Med 1996; 184:2049–2053